

# ECATS: Explainable-by-design concept-based anomaly detection for time series

Irene Ferfaglia<sup>1</sup>[0000-0003-1585-6576], Gaia Saveri<sup>1,2</sup>[0009-0003-2948-7705],  
Laura Nenzi<sup>1</sup>[0000-0003-2263-9342], and Luca Bortolussi<sup>1</sup>[0000-0001-8874-4001]

<sup>1</sup> Università degli Studi di Trieste, Italy

<sup>2</sup> Università degli Studi di Pisa, Italy

**Abstract.** Deep learning methods for time series have already reached excellent performances in both prediction and classification tasks, including anomaly detection. However, the complexity inherent in Cyber Physical Systems (CPS) creates a challenge when it comes to explainability methods. To overcome this inherent lack of interpretability, we propose ECATS, a concept-based neuro-symbolic architecture where concepts are represented as Signal Temporal Logic (STL) formulae. Leveraging kernel-based methods for STL, concept embeddings are learnt in an unsupervised manner through a cross-attention mechanism. The network makes class predictions through these concept embeddings, allowing for a meaningful explanation to be naturally extracted for each input. Our preliminary experiments with a simple CPS-based dataset show that our model is able to achieve great classification performance while ensuring local interpretability.

**Keywords:** CPS · Anomaly detection · STL · Concept-based learning

## 1 Introduction

Cyber-physical systems (CPS) are commonly used for the monitoring and controlling of industrial processes in important assets such as power grids, water treatment facilities, and autonomous vehicles. The monitoring of the sensor readings in such systems is critical for early detection of unexpected system behaviour as it allows for timely attenuating actions - such as fault checking, predictive maintenance, and system shutdown - to be taken, such that potential problem caused by system failures can be avoided. The increasing complexity of modern CPS has made traditional anomaly detection mechanisms insufficient. Consequently, the use of machine learning and deep learning algorithms has become a clear direction to build data-driven anomaly detection frameworks.

The signals of a CPS are mainly time series data that are continuously recorded over time. While deep learning models have been able to correctly predict the presence of an anomaly in time series [6], most methods do so in a black-box manner. Lack of transparency in the decision process is a characteristic of many deep learning models. This creates a deficiency of human trust despite their state-of-the-art performance across most tasks [18], raising

ethical [12,13] and legal [8,11] concerns. Specifically, anomaly detection is critical for maintaining CPS' integrity and functionality and can greatly benefit from an interpretable model to guide the work.

Indeed, explainability is now an important research topic in the field of AI [21]. Historically, a large part of the work in explainability is done on tabular data [24] or in the field of computer vision [3], where deep neural networks (DNN) typically achieve state-of-the-art performance. The research field of eXplainable AI (XAI) for trajectory classification has seen a surge of attention since 2019 [23,27]. Common explainability methods for time series are based on Convolutional Neural Networks (CNN), articulating in backpropagation-based methods [26,31,34] and perturbation-based methods [15]. The other common approach for XAI methods in time series is coming from Natural Language Processing (NLP) and is rooted in the attention mechanism [9,14,29].

On the other hand, concept-based models are designed to increase explainability in deep learning models by exploiting more human-understandable concepts to describe their decision process. This can be done using methods such as logistic regression or decision trees [16,17] or, as the latest state-of-the-art, concept embeddings. However, currently, most of these methods focus on the classification of images [4,30], tabular data [33], or graphs [1], leaving a gap to fill in terms of trajectory data.

In this paper, we propose ECATS, the first interpretable neuro-symbolic concept-based model for trajectories. It uses a cross-attention-based network to perform binary classification on some potentially anomalous trajectories by leveraging STL formulae as concepts and exploiting their properties.

## 2 Preliminaries

**Concept-based models** Recent work on explainable AI introduces this novel type of explanation approach [10,32], providing human-understandable concepts as explanations for the predictions rather than the relative importance of input features, better resonating with human reasoning. Explainable-by-design concept-based models depart from standard neural networks by explicitly incorporating a set of concepts within the architecture, which can be provided as part of the dataset or computed by the model itself.

**Signal Temporal Logic** Signal Temporal Logic (STL) is a formalism used in formal verification and synthesis of CPS. STL formulae describe relationships between signals over dense time intervals, allowing us to express properties such as "the temperature should never exceed a certain threshold for more than a specified duration". Besides classical propositional logic operators, STL syntax is endowed with *temporal* operators eventually, globally and until, decorated with time intervals  $[a, b]$ . They can be intuitively interpreted as: a property is *eventually* satisfied if it is satisfied at some point inside the temporal interval, while a property is *globally* satisfied if it is true continuously in  $[a, b]$ ; finally the *until* operator captures the relationship between two conditions  $\varphi, \psi$  in which the first condition  $\varphi$  holds until, at some point in  $[a, b]$ , the second

condition  $\psi$  becomes true. Notably, STL is endowed with both *qualitative* (or Boolean) semantics, giving the classical notion of satisfaction of a property over a trajectory, and a *quantitative* semantics (or *robustness*)  $\rho(\varphi, \xi)$ , which is a measure of how robust is the satisfaction of  $\varphi$  w.r.t. perturbations of the signal  $\xi$ . A formal definition of STL syntax and semantics is given in Appendix A.

**A kernel for STL formulae** Finding continuous representations of STL formulae is performed with an ad hoc kernel in [2], by leveraging the quantitative semantics of STL. Indeed, robustness allows formulae to be considered as functionals mapping trajectories into real numbers, i.e.  $\rho(\varphi, \cdot) : \mathcal{T} \rightarrow \mathbb{R}$  such that  $\xi \mapsto \rho(\varphi, \xi)$ . Considering these as feature maps, and fixing a probability measure  $\mu_0$  on the space of trajectories  $\mathcal{T}$ , a kernel function capturing similarity among STL formulae can be defined as:

$$k(\varphi, \psi) = \langle \rho(\varphi, \cdot), \rho(\psi, \cdot) \rangle = \int_{\xi \in \mathcal{T}} \rho(\varphi, \xi) \rho(\psi, \xi) d\mu_0(\xi) \quad (1)$$

opening the doors to the use of the scalar product in the Hilbert space  $L^2$  as a kernel for  $\mathcal{P}$ , the space of parameters. Intuitively, this results in a kernel having a high positive value for formulae that behave similarly on high-probability trajectories (w.r.t.  $\mu_0$ ) and, vice versa, low negative value for formulae that on those trajectories disagree. Finite-dimensional embeddings can be recovered by kernel PCA [25]. More details about the kernel can be found in Appendix B.

### 3 ECATS architecture

Here we describe ECATS (Explainable-by-design Concept-based Anomaly detection model for Time Series), the first interpretable neuro-symbolic concept-based model for trajectories. The goal of our proposed methodology is to discriminate between normal and anomalous signals, contextually providing an explanation for the outcome. In particular, the form of the explanation is a disjunction of interpretable STL formulae, which act as concepts in our model, whose semantics is influential for determining the label of the input trajectory. Indeed, as mentioned in Section 2, STL is a concise yet rich language to describe the characteristics of time series, and therefore is a valuable candidate to serve as a concept language in this field. In fact, small STL formulae describe simple patterns in a signal, and are easy to understand for a human (possibly once converted into a natural language description).

We now describe at a high level how the model works. We provide Figure 1 as a reference to graphically follow the discussion. Our model takes as input a signal  $\xi$  and, through a mechanism of cross-attention (Subsection 3.1) between a kernel embedding of the concepts (computed as per Equation 1) and the input trajectory, creates an efficient representation of the relationship between the two. The end product gets fed to an MLP classifier net, which outputs its prediction  $y$ , the class of the input trajectory. Our model is then able to provide not only excellent classification accuracy (Section 4), but also easy-to-read explanations made of simple STL formulae (Subsection 3.2).

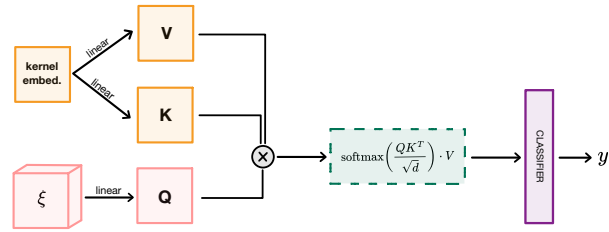


Fig. 1: Architecture of ECATS.  $V, K, Q$  are respectively the values, keys and query matrices typical of an attention mechanism.

### 3.1 Cross-attention

Since its introduction, self-attention [28] has been widely used in many different forms to enhance feature representations. By simulating how human attention works and assigning varying levels of importance to different parts of the input, a model implementing attention is able to weight the importance of each element in the input concerning all other elements.

While self-attention captures relationships within a single input sequence, cross-attention [5] captures the relationships between elements of two different input sequences, allowing the model to generate coherent and contextually relevant outputs. Applied to our case, cross-attention allows us to take a trajectory and compute its attention values with respect to a kernel embedding of a fixed dataset of STL formulae. We selected the set of formulae  $\mathcal{C}$  to be used as concepts with a procedure aimed at maximising the coverage of the semantic space of the formulae and avoiding semantic redundancies, namely sampling from the latent space defined by the STL kernel and inverting the embeddings to identify the corresponding formulae (in fact, simple formulae with a very close embedding). For more details, see Appendix C. The use of cross-attention produces an attention matrix which will be used also when retrieving an explanation for the output of our model, other than for prediction.

### 3.2 Concept-based explanation

*Local explanations* can be extracted for the output of each classified trajectory. Given a set of concepts  $\mathcal{C}$  identified as described above, we aim to explain the model prediction for a given input trajectory  $\xi$ . The explanation can be expressed as a subset of  $\mathcal{C}$ , i.e.  $\mathcal{E} \subseteq \mathcal{C}$ , where each formula  $\varphi \in \mathcal{E}$  is associated with its robustness  $\rho(\varphi, x)$  w.r.t. the input trajectory and its attention weight computed through a forward pass. Robustness helps determine the role that  $\varphi$  played in the classification (i.e. if they are positive or negative witnesses). For more information on the robustness, see Appendix A.

The formulae are then ranked by their attention weight and can be filtered by kernel similarity (see Appendix C) to obtain a more meaningful subset of formulae. The final explanation is the conjunction of the contents of the subset.

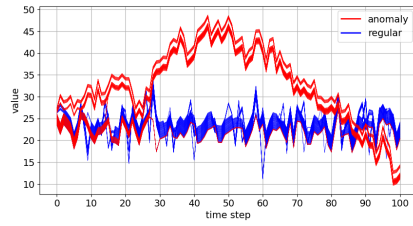


Fig. 2: Representation of the classes in the train cruise control dataset.

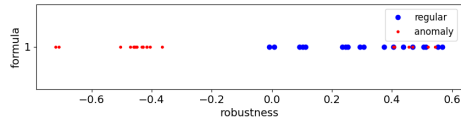


Fig. 3: Robustness of global explanation for anomalous trajectories' class.

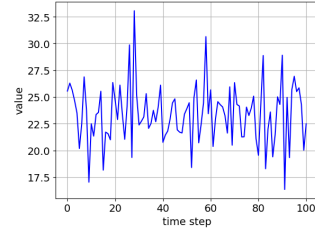


Fig. 4: An example of regular trajectory.

*Global explanations* by class, can be easily extracted from local ones. In general, each local explanation may have different weights and concepts. However, we can still globally interpret the predictions of our model without the need for an external post-hoc explainer. To achieve this, we collect the batch of unfiltered formulae produced as explanation for each trajectory of a class with the highest attention value. We then filter this batch by kernel similarity to finally obtain a handful of STL formulae able to characterise the class they refer to.

A *post-processing step* is applied to improve human readability and comprehension. While the model may be able to distinguish between classes with a given formula, the separation may not be intuitive to the human eye. So, a given formula's threshold is shifted in a way that it becomes true for a class, and false for the other, i.e. opposite signs of robustness. If the formula is given an explanation for a trajectory or a class for which it is false, the formula gets negated in order to invert the roles and become true for the element in focus. They can be condensed into a single formula by disjunction. See Appendix D for details.

## 4 Experiments

**Setup** We evaluate ECATS on a train cruise control dataset proposed by [22], and use the standard training/test split. The dataset, balanced between classes, collects 200 trajectories of 1 dimension and has a clear-cut condition to classify between regular and anomalous trajectories, except for seven outliers. In Figure 2, a visual representation of the dataset.

**Evaluation** To assess the classification performance of our model, we run the tests using 5 different initialisation seeds. This shows that its classification accuracy averages at 96.5%, with a standard deviation of 2.55. Following, some example outputs from ECATS, starting from a local explanation. Consider the post-processed explanation given for a signal  $\xi$  correctly classified as regular:

$$\neg (\xi \leq 35.9 \mathcal{U}_{[11,36]} \xi \geq 31.5)$$

The first part of the formula,  $\xi \leq 35.9$ , is true for almost all trajectories, no matter the class. However, the second part,  $\xi \geq 31.5$ , is not true for regular classes, making the formula inside the parentheses false for the considered signal. This is backed by the robustness of this STL formula on the trajectory, namely  $-0.55$ . With the negation, its robustness becomes positive and the formula becomes true for the regular class and helps indeed discriminate between regular and anomalous trajectories while characterising the studied signal.

Here is an example of post-processed global explanations given by ECATS:

$$\text{Regular: } \neg (\xi \geq 20.0 \mathcal{U}_{[23,47]} \xi \leq 40.5)$$

$$\text{Anomaly: } \neg \mathcal{G}_{[0,24]} \xi \leq 28.7$$

In Figure 3, the robustness values for the formula given as explanation for the anomalous class, computed for all trajectories. Except for some points which are most likely the aforementioned outliers, the class separation is linear. For training details and further discussion of results, we refer to Appendix E.

## 5 Conclusions

We introduced ECATS, a pioneering interpretable neuro-symbolic concept-based model designed specifically for the classification of trajectory data in CPS. By leveraging STL formulae as concepts and using a cross-attention-based network, we proved that our model is able to provide not only accurate anomaly detection but also transparent and human-understandable explanations, giving insight into the decision-making processes. This not only facilitates timely and appropriate responses to potential system failures but also promotes greater user confidence in the model’s predictions.

A significant strength of our approach is its versatility in various practical scenarios. Thanks to ECATS’ ability to provide not only global but also local explanations, it can be effectively applied even in cases where: i) a labeled dataset is not available, ii) only semi-supervised data is present, iii) there is minimal prior knowledge about the data, or iv) the amount of data is limited. This flexibility makes ECATS a robust solution for a wide range of real-world applications where data constraints and uncertainties are common.

*Future work* will aim to extend this model capabilities to multivariate trajectories and investigate the potential integration of additional explainability techniques to further enhance its utility and effectiveness. Lastly, further automatic post-processing of the explanations is needed in order to provide even more clear and understandable STL formulae.

## References

1. Barbiero, P., Ciravegna, G., Giannini, F., Zarlenga, M.E., Magister, L.C., Tonda, A., Lio, P., Precioso, F., Jarnik, M., Marra, G.: Interpretable neural-symbolic concept reasoning. In: Krause, A., Brunskill, E., Cho, K., Engelhardt, B., Sabato, S., Scarlett, J. (eds.) International Conference on Machine Learning, ICML 2023, 23-29 July 2023, Honolulu, Hawaii, USA. Proceedings of Machine Learning Research, vol. 202, pp. 1801–1825. PMLR (2023)
2. Bortolussi, L., Gallo, G.M., Kretínský, J., Nenzi, L.: Learning model checking and the kernel trick for signal temporal logic on stochastic processes. In: Tools and Algorithms for the Construction and Analysis of Systems - 28th International Conference, TACAS 2022, Proceedings, Part I (2022)
3. Buhrmester, V., Münch, D., Arens, M.: Analysis of explainers of black box deep neural networks for computer vision: A survey. *Machine Learning and Knowledge Extraction* **3**(4), 966–989 (2021)
4. Chen, C., Li, O., Tao, C., Barnett, A.J., Su, J., Rudin, C.: This looks like that: Deep learning for interpretable image recognition (2019)
5. Chen, C.F., Fan, Q., Panda, R.: Crossvit: Cross-attention multi-scale vision transformer for image classification (2021)
6. Darban, Z.Z., Webb, G.I., Pan, S., Aggarwal, C.C., Salehi, M.: Deep learning for time series anomaly detection: A survey (2022)
7. Donzé, A., Ferrère, T., Maler, O.: Efficient robust monitoring for stl. vol. 8044 (07 2013). [https://doi.org/10.1007/978-3-642-39799-8\\_19](https://doi.org/10.1007/978-3-642-39799-8_19)
8. European Commission: Regulation (EU) 2016/679 of the European Parliament and of the Council of 27 April 2016 on the protection of natural persons with regard to the processing of personal data and on the free movement of such data, and repealing Directive 95/46/EC (General Data Protection Regulation) (Text with EEA relevance) (2016), <https://eur-lex.europa.eu/eli/reg/2016/679/oj>
9. Ge, W., Huh, J.W., Park, Y.R., Lee, J.H., Kim, Y.H., Turchin, A.: An interpretable icu mortality prediction model based on logistic regression and recurrent neural networks with lstm units. In: AMIA Annual Symposium Proceedings. vol. 2018, p. 460. American Medical Informatics Association (2018)
10. Ghorbani, A., Wexler, J., Zou, J., Kim, B.: Towards automatic concept-based explanations (2019)
11. Helbing, D.: Societal, Economic, Ethical and Legal Challenges of the Digital Revolution: From Big Data to Deep Learning, Artificial Intelligence, and Manipulative Technologies, pp. 47–72. Springer International Publishing, Cham (2019). [https://doi.org/10.1007/978-3-319-90869-4\\_6](https://doi.org/10.1007/978-3-319-90869-4_6)
12. Ho, A.: Deep ethical learning: Taking the interplay of human and artificial intelligence seriously. The Hastings Center report **49**, 36–39 (02 2019). <https://doi.org/10.1002/hast.977>
13. Iman, M., Arabnia, H.R., Branchinst, R.M.: Pathways to artificial general intelligence: A brief overview of developments and ethical issues via artificial intelligence, machine learning, deep learning, and data science. In: Arabnia, H.R., Ferens, K., de la Fuente, D., Kozerenko, E.B., Olivas Varela, J.A., Tinetti, F.G. (eds.) Advances in Artificial Intelligence and Applied Cognitive Computing. pp. 73–87. Springer International Publishing, Cham (2021)
14. Karim, F., Majumdar, S., Darabi, H., Chen, S.: Lstm fully convolutional networks for time series classification. *IEEE Access* **6**, 1662–1669 (2018). <https://doi.org/10.1109/access.2017.2779939>, <http://dx.doi.org/10.1109/ACCESS.2017.2779939>

15. Kashiparekh, K., Narwariya, J., Malhotra, P., Vig, L., Shroff, G.: ConvTimentet: A pre-trained deep convolutional neural network for time series classification (2019)
16. Kazhdan, D., Dimanov, B., Jamnik, M., Liò, P., Weller, A.: Now you see me (cme): Concept-based model extraction (2020)
17. Koh, P.W., Nguyen, T., Tang, Y.S., Mussmann, S., Pierson, E., Kim, B., Liang, P.: Concept bottleneck models. In: III, H.D., Singh, A. (eds.) Proceedings of the 37th International Conference on Machine Learning. Proceedings of Machine Learning Research, vol. 119, pp. 5338–5348. PMLR (13–18 Jul 2020), <https://proceedings.mlr.press/v119/koh20a.html>
18. Leichtmann, B., Humer, C., Hinterreiter, A., Streit, M., Mara, M.: Effects of explainable artificial intelligence on trust and human behavior in a high-risk decision task. *Computers in Human Behavior* **139**, 107539 (2023). <https://doi.org/https://doi.org/10.1016/j.chb.2022.107539>
19. Maler, O., Nickovic, D.: Monitoring temporal properties of continuous signals. vol. 3253, pp. 152–166 (01 2004). [https://doi.org/10.1007/978-3-540-30206-3\\_12](https://doi.org/10.1007/978-3-540-30206-3_12)
20. Mohammadinejad, S., Deshmukh, J.V., Puranic, A.G., Vazquez-Chanlatte, M., Donzé, A.: Interpretable classification of time-series data using efficient enumerative techniques. In: HSCC '20: 23rd ACM International Conference on Hybrid Systems: Computation and Control. pp. 9:1–9:10. ACM (2020)
21. Nagahisarchoghaei, M., Nur, N., Cummins, L., Nur, N., Karimi, M.M., Nandanwar, S., Bhattacharyya, S., Rahimi, S.: An empirical survey on explainable ai technologies: Recent trends, use-cases, and categories from technical and application perspectives. *Electronics* **12**(5) (2023). <https://doi.org/10.3390/electronics12051092>
22. Pigozzi, F., Nenzi, L., Medvet, E.: BUSTLE: a Versatile Tool for the Evolutionary Learning of STL Specifications from Data. *Evolutionary Computation* pp. 1–24 (02 2024). [https://doi.org/10.1162/evco\\_a\\_00347](https://doi.org/10.1162/evco_a_00347)
23. Rojat, T., Puget, R., Filliat, D., Ser, J.D., Gelin, R., Díaz-Rodríguez, N.: Explainable artificial intelligence (xai) on timeseries data: A survey (2021)
24. Sahakyan, M., Aung, Z., Rahwan, T.: Explainable artificial intelligence for tabular data: A survey. *IEEE Access* **9**, 135392–135422 (2021). <https://doi.org/10.1109/ACCESS.2021.3116481>
25. Schölkopf, B., Smola, A.J., Müller, K.: Kernel principal component analysis. In: ICANN '97, 7th International Conference, Lausanne, Switzerland, October 8-10, 1997, Proceedings. Lecture Notes in Computer Science, vol. 1327, pp. 583–588. Springer (1997)
26. Strodthoff, N., Strodthoff, C.: Detecting and interpreting myocardial infarction using fully convolutional neural networks. *Physiological Measurement* **40**(1), 015001 (Jan 2019). <https://doi.org/10.1088/1361-6579/aaf34d>, <http://dx.doi.org/10.1088/1361-6579/aaf34d>
27. Theissler, A., Spinnato, F., Schlegel, U., Guidotti, R.: Explainable ai for time series classification: A review, taxonomy and research directions. *IEEE Access* **10**, 100700–100724 (2022). <https://doi.org/10.1109/ACCESS.2022.3207765>
28. Vaswani, A., Shazeer, N., Parmar, N., Uszkoreit, J., Jones, L., Gomez, A.N., Kaiser, L., Polosukhin, I.: Attention is all you need (2023)
29. Vinayavekhin, P., Chaudhury, S., Munawar, A., Agravante, D.J., Magistris, G.D., Kimura, D., Tachibana, R.: Focusing on what is relevant: Time-series learning and understanding using attention (2018)
30. Wang, B., Li, L., Nakashima, Y., Nagahara, H.: Learning bottleneck concepts in image classification (2023)

31. Wang, Z., Yan, W., Oates, T.: Time series classification from scratch with deep neural networks: A strong baseline (2016)
32. Yeh, C.K., Kim, B., Arik, S., Li, C.L., Pfister, T., Ravikumar, P.: On completeness-aware concept-based explanations in deep neural networks. In: Larochelle, H., Ranzato, M., Hadsell, R., Balcan, M., Lin, H. (eds.) *Advances in Neural Information Processing Systems*. vol. 33, pp. 20554–20565. Curran Associates, Inc. (2020)
33. Zarlenga, M.E., Barbiero, P., Ciravegna, G., Marra, G., Giannini, F., Diligenti, M., Shams, Z., Precioso, F., Melacci, S., Weller, A., Lio, P., Jarnik, M.: *Concept embedding models: Beyond the accuracy-explainability trade-off* (2022)
34. Zhou, B., Khosla, A., Lapedriza, A., Oliva, A., Torralba, A.: *Learning deep features for discriminative localization* (2015)

## Appendix A Signal Temporal Logic

Signal Temporal Logic (STL) [19] is a formal specification language to express temporal properties over real-value trajectories with a dense time interval. We now present its syntax and semantics.

For the rest of the paper, let be  $\xi : \mathcal{T} \rightarrow \mathbb{R}^n$  a trajectory, where  $\mathcal{T} = \mathbb{R} \geq 0$  is the time domain,  $\xi_i(t)$  is the value at time  $t$  of the projection on the  $i$ -th coordinate, and  $\xi = (\xi_1, \dots, \xi_n)$ , as an abuse on the notation, is used also to indicate the set of variables of the trace considered in the formulae.

**Definition 1.** *The syntax of STL is given by*

$$\varphi := \top \mid \mu \mid \neg\varphi \mid \varphi_1 \wedge \varphi_2 \mid \phi_1 \mathcal{U}_I \varphi_2$$

where  $\top$  is the Boolean true constant, negation  $\neg$  and conjunction  $\wedge$  are the standard Boolean connectives, and  $\mathcal{U}_I$  is the Until temporal modality, where  $I$  is a real positive interval. We can derive the disjunction operator  $\vee$ , the future eventually  $\mathcal{F}_I$  and always  $\mathcal{G}_I$  operators from the until temporal modality ( $\varphi_1 \vee \varphi_2 = \neg(\neg\varphi_1 \wedge \neg\varphi_2)$ ,  $\mathcal{F}_I\varphi = \top \mathcal{U}_I\varphi$ ,  $\mathcal{G}_I\varphi = \neg\mathcal{F}_I\neg\varphi$ ).

STL can be interpreted over a trajectory  $\xi$  using a qualitative or a quantitative semantics [7]. The quantitative satisfaction function  $\rho$  returns a value  $\rho(\varphi, x, t) \in \bar{\mathbb{R}}^3$  quantifying the *robustness degree* of the property  $\varphi$  by the trajectory  $\xi$  at time  $t$ . Its sign provides the link with the standard Boolean semantics in that a signal  $\xi$  satisfies an STL formula  $\varphi$  at a time  $t$  iff the robustness degree  $\rho(\varphi, \xi, t) \geq 0$ . Its absolute value, instead, can be interpreted as a measure of the robustness of the satisfaction with respect to noise in signal  $\xi$ , measured in terms of the maximal perturbation in the secondary signal  $\theta(\xi(t))$ , preserving

<sup>3</sup>  $\bar{\mathbb{R}} = \mathbb{R} \cup \{-\infty, +\infty\}$

truth value. Robustness is recursively defined as:

$$\begin{aligned}
\rho(\pi, \xi, t) &= f_\pi(\xi(t)) && \text{for } \pi(\mathbf{x}) = (f_\pi(\mathbf{x}) \geq 0) \\
\rho(\neg\varphi, \xi, t) &= -\rho(\varphi, \xi, t) \\
\rho(\varphi_1 \wedge \varphi_2, \xi, t) &= \min(\rho(\varphi_1, \xi, t), \rho(\varphi_2, \xi, t)) \\
\rho(\varphi_1 \mathbf{U}_{[a,b]} \varphi_2, \xi, t) &= \max_{t' \in [t+a, t+b]} (\min(\rho(\varphi_2, \xi, t'), \min_{t'' \in [t, t']} \rho(\varphi_1, \xi, t'')))
\end{aligned}$$

For completeness, we report also the definition of robustness of derived temporal operators: eventually  $\rho(\mathbf{F}_{[a,b]}\varphi, \xi, t) = \max_{t' \in [t+a, t+b]} \rho(\varphi, \xi, t')$  and globally  $\rho(\mathbf{G}_{[a,b]}\varphi, \xi, t) = \min_{t' \in [t+a, t+b]} \rho(\varphi, \xi, t')$ . Robustness is compatible with satisfaction via the following *soundness* property: if  $\rho(\varphi, \xi, t) > 0$  then  $s(\varphi, \xi, t) = 1$  and if  $\rho(\varphi, \xi, t) < 0$  then  $s(\varphi, \xi, t) = 0$ . When  $\rho(\varphi, \xi, t) = 0$  arbitrary small perturbations of the signal might lead to changes in satisfaction value. We omit  $t$  from the previous notation when the properties are evaluated at time  $t = 0$ .

## Appendix B STL Kernel

In what follows, we provide details on the measure  $\mu_0$  used in the space of trajectories, to get a more intuitive understanding of the kernel for STL formulae defined in Section 2 (and, in particular, Equation 1).

---

**Algorithm 1** Sampling a trajectory over the interval  $[a, b]$  according to  $\mu_0$

---

**Input:**  $\Delta, a, b, m', m'', \sigma', \sigma'', q$

**Output:**  $\xi$

▷ sample the starting point

$\xi_0 \sim \mathcal{N}(m', \sigma')$

$\xi(t_0) \leftarrow \xi_0$

▷ sample the total variation

$K \sim (\mathcal{N}(m'', \sigma''))^2$

$y_1, \dots, y_{N-1} \sim \mathbb{U}([0, K])$

$y_0 \leftarrow 0, y_n \leftarrow K$

orderAndRename( $y_0, \dots, y_n$ )

▷ now  $y_1 \leq y_2 \leq \dots \leq y_{N-1}$

$s_0 \sim \text{Discr}(-1, 1)$

**while**  $i \leq N$  **do**

$s \leftarrow \text{Binomial}(q)$

▷  $P(s = -1) = q$

$s_{i+1} = s_i \cdot s$

$\xi(t_{i+1}) = \xi(t_i) + s_{i+1}(y_{i+1} - y_i)$

**end while**

---

Intuitively,  $\mu_0$  makes *simple* trajectories more probable, considering total variation and number of changes in monotonicity as indicators of complexity of

**Algorithm 2** Algorithms for generating STL formulae templates

---

**Input:**  $M, N$   
**Output:** all\_phis  $\triangleright$  STL templates of formulae with max  $N$  vars and  $M$  nodes  
all\_phis  $\leftarrow \emptyset$   
all\_phis.append(generateAtomicPropositions())  $\triangleright x_i \leq 0$  or  $x_i \geq 0, \forall i \leq N$   
**for**  $2 \leq m \leq M$  **do**  
prev\_phis  $\leftarrow$  getPhisGivenNodes( $m - 1$ )  $\triangleright$  retrieve templates with  $m - 1$  nodes  
unary\_ops  $\leftarrow$  expandByUnaryOperators(prev\_phis)  $\triangleright F, G, \neg$   
all\_phis.append(unary\_ops)  
l\_list, r\_list  $\leftarrow$  getPairsGivenSum( $m$ )  $\triangleright$  all pairs  $(l, r) : l + r = m, l \leq r$   
**for**  $(l, r) \in [l\_list, r\_list]$  **do**  
l\_phis  $\leftarrow$  getPhisGivenNodes( $l$ )  
r\_phis  $\leftarrow$  getPhisGivenNodes( $r$ )  
binary\_ops  $\leftarrow$  expandByBinaryOperators(l\_phis, r\_phis)  $\triangleright \wedge, \vee, U$   
all\_phis.append(binary\_ops)  
**end for**  
**end for**

---

signals. The measure  $\mu_0$ , operating on piecewise linear functions over the interval  $\mathcal{I} = [a, b]$  (which is a dense subset of the set of continuous functions over  $\mathcal{I}$ ), can be algorithmically defined as in Algorithm 1 (default parameters are set as  $a = 0, b = 100, \Delta = 1, m' = m'' = 0'', \sigma' = \sigma'' = 1, q = 0.1$ ). Note that although the feature space  $\mathbb{R}^{\mathcal{T}}$  into which  $\rho$  (and thus Equation (1)) maps formulae is infinite-dimensional, in practice the kernel trick allows to circumvent this issue by mapping each formula to a vector of dimension equal to the number of formulae which are in the training set used to evaluate the kernel (Gram) matrix.

## Appendix C Selecting the concepts

We construct the STL formulae used as concepts by fixing the maximum number  $M$  of nodes and the maximum number of variables  $N$  (i.e. the dimensionality of the input signals) allowed, then we enumerate all templates (i.e., STL formulae where constants are replaced by parameters) satisfying those constraints as detailed in Algorithm 2.

Once all the templates have been generated, we instantiate each of them on a set of parameter configurations  $\mathcal{P} = \{p_0, \dots, p_{|\mathcal{P}|}\}$  to be filtered by Signature-based Optimisation as defined in [20]. Denoting as  $\varphi(p)$  the application of the parameter set  $p$  to the template formula  $\varphi$ , and given a set of trajectories  $\hat{\mathcal{T}} = \{\xi_0, \dots, \xi_{|\hat{\mathcal{T}}|}\}$  (with  $p \in \mathcal{P}$ , and  $\hat{\mathcal{T}} \subset \mathcal{T}$ ), it consists in building a matrix  $S \in \mathbb{R}^{|\mathcal{P}| \times |\hat{\mathcal{T}}|}$ , whose rows are called the *signature* of the formula, s.t.  $S(i, j) = \rho(\varphi(p_i), \xi_j)$ , i.e. the cell  $(i, j)$  of such matrix holds the robustness of the  $i$ -th instantiation of  $\varphi$  on the  $j$ -th trajectory. In such matrix, the distance between rows can be considered as a proxy for semantic similarity among different parameterisations of the same template, hence a selection on formulae can be done by keeping only those whose signature has a distance higher than a certain threshold  $\tau \in \mathbb{R}_{\geq 0}$  from formulae already selected. This helps in

removing redundancy in the set of concepts. In our case, we use signature-based optimisation with cosine distance and threshold  $\tau = 0.9$  and, for interpretability, we keep  $M$  fairly small, namely  $M = 3$ .

### C.1 Latin Hypercube Sampling

Latin Hypercube Sampling (LHS) was used in order to sample a meaningful subset of concepts of size  $m$  from their kernel embedding. LHS is a type of stratified Monte Carlo method developed in the 1970s employed to efficiently sample from multidimensional spaces, including matrices. Unlike traditional random sampling methods, LHS ensures a more uniform coverage of the space. By partitioning the range of each component into equally probable intervals and selecting one sample from each interval per component, LHS mitigates the risk of oversampling certain regions while neglecting others, thereby minimising biases inherent in the sampling process. In our case, we selected a pool of  $m = 5000$  concepts.

## Appendix D Post-processing of explanations

As mentioned in Section 4, although being able to accurately distinguish between classes, STL formulae provided by the model as explanations are not optimised towards their human-understandability. In particular, one would expect the robustness of such formulae to be positive (indicating boolean satisfaction) on trajectories belonging to the class they describe, and negative for signals belonging to the opposite class. This can be obtained without altering the discriminative power of the formula by shifting of a fixed quantity  $\varepsilon$  all the variable thresholds appearing in the explanation. A trivial way to do so is by trying an arbitrary number of values for  $\varepsilon$  (e.g. choosing from a grid of candidates), and keeping the smallest one for which the sign of the robustness is the same for all trajectory belonging to a class, and the opposite for all trajectories belonging to the other. Finally, to achieve the property of having positive robustness on signals of the class pertaining the explanation, one can simply negate the formula. Putting together these post-processing steps transform the original explanation (without changing its separation properties), hence it might be the case that a syntactic simplification is possible, enhancing human readability of the explanation, keeping its semantic untouched (i.e. just applying logical equivalences). Notably, all these post-processing steps can be performed automatically.

## Appendix E Training setup and results

The model was trained for 50 epochs with a Binary Cross Entropy (BCE) loss and  $1e^{-5}$  learning rate, with 5 different initialisation seeds. We here report and further discuss the results obtained with one of the seeds.

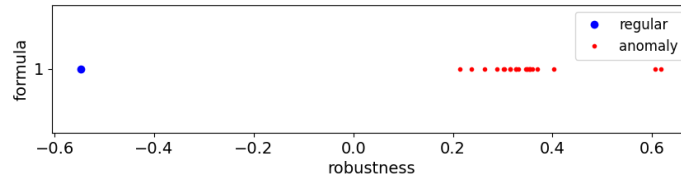


Fig. 5: Robustness values for the explanation of the regular trajectory reported as example in Section 4.

First, we better analyse the local explanation for a regular trajectory outlined in Section 4 by reporting the plot of the robustness values for the considered signal versus all the signals of the opposite class (Figure 5). For ease, we report here the provided explanation:

$$\neg (\xi \leq 35.9 \mathcal{U}_{[11,36]} \xi \geq 31.5)$$

A per Figure 5, the provided formula does an excellent job at separating the signal belonging to the regular class from the ones that are anomalous. Coincidentally the cluster of values regarding the anomalous class has opposite sign with respect to the robustness on the considered regular signal, therefore the formula has no need to be shifted to increase human readability.

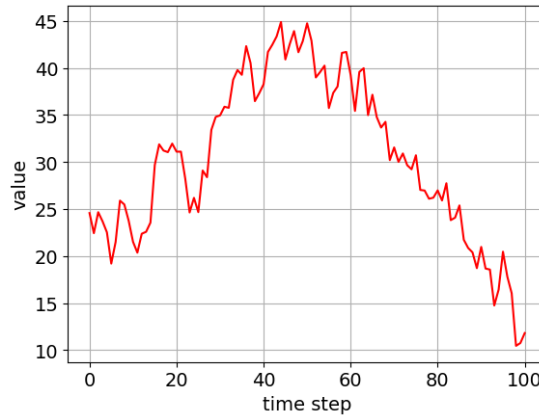


Fig. 6: An example of anomalous trajectory.

However, this is not always the case. We now report a local explanation for an anomalous trajectory, represented in Figure 6. The original provided explanation is the following.

$$\mathcal{G}_{[0,24]} \xi \leq 37.3$$

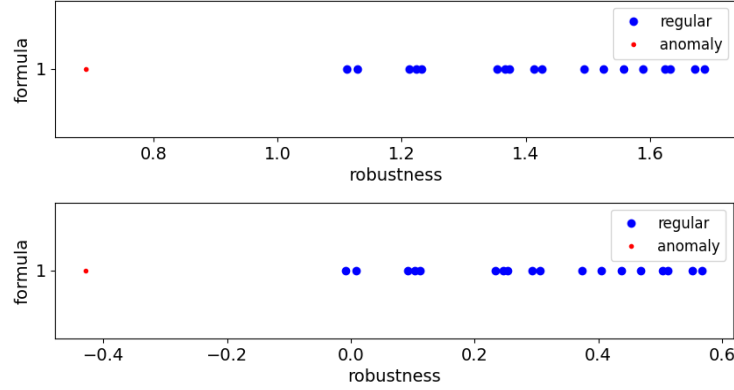


Fig. 7: Robustness values for the explanation of the anomalous trajectory reported as example, before (top) and after (bottom) postprocessing.

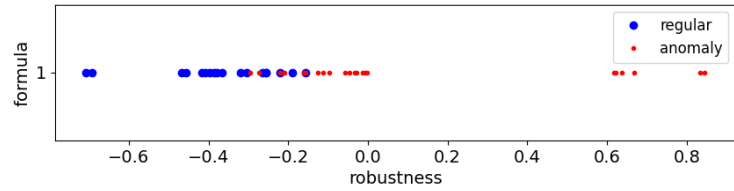


Fig. 8: Robustness of global explanation for regular trajectories' class.

Indeed, also from Figure 2 one can assess that the formula is true for all trajectories in the dataset. This is not an intuitive explanation, but we can see from the corresponding robustness plot (Figure 7, top) that it does in fact separate the two classes. So, we can shift the values in the formula, obtaining the following post-processed explanation and robustness values of inverse sign (Figure 7, bottom):

$$\neg \mathcal{G}_{[0,24]} \xi \leq 28.7$$

See Appendix D for more details on the simplification of formulae.

We now recall the global explanation by class reported in Section 4:

$$\begin{aligned} \text{Regular: } & \neg (\xi \geq 20.0 \mathcal{U}_{[23,47]} \xi \leq 40.5) \\ \text{Anomaly: } & \neg \mathcal{G}_{[0,24]} \xi \leq 28.7 \end{aligned}$$

and report here the plot for the robustness values of the explanation for the regular class (Figure 8), in order to integrate the one already reported in Section 4, Figure 3. As mentioned earlier, Except for a few points which are most likely the outliers, the separation between classes is clear.